Article

pubs.acs.org/Biomac

Biophysical Properties and Supramolecular Structure of Self-Assembled Liposome/ε-Peptide/DNA Nanoparticles: Correlation with Gene Delivery

Jiang Yan, Nikolay Korolev, Khee Dong Eom, James P. Tam, and Lars Nordenskiöld*

School of Biological Sciences, Nanyang Technological University, 60 Nanyang Drive, Singapore, 637551

Supporting Information

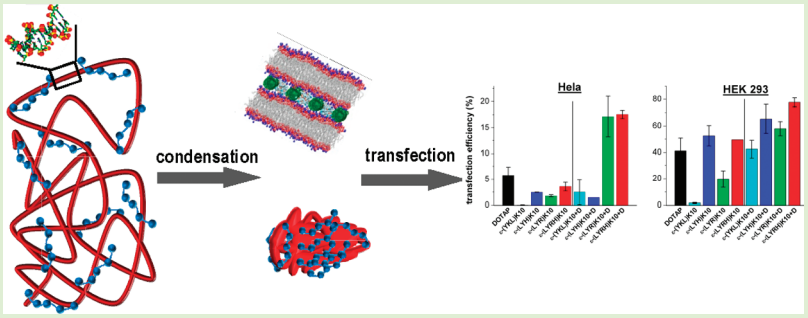

ABSTRACT: Using solid-phase synthesis, lysine can be oligomerized by a reaction of the peptide carboxylate with the ε-amino group to produce nontoxic, biodegradable cationic peptides, ε-oligo(L-lysines). Here α-substituted derivatives of such ε-oligo-(L-lysines) containing arginine and histidine in the side chain were tested as vectors for in vitro gene delivery. Combination of ε-oligolysines with the cationic lipid DOTAP and plasmid DNA resulted in transfection efficiency exceeding that of DOTAP alone, without significant increase in cytotoxicity. Synchrotron small-angle X-ray scattering studies revealed self-assembly of the DOTAP, ε-oligolysines, and DNA to ordered lamellar complexes. High transfection efficiency of the nanoparticles correlates with increase in zeta potential above +20 mV and requires particle size to be below 500 nm. The synergistic effect of branched ε-oligolysines and DOTAP in gene delivery can be explained by the increase in surface charge and by the supramolecular structure of the DOTAP/ε-oligolysine/DNA nanoparticles.

INTRODUCTION

Recently, the development of synthetic vectors that condense plasmid DNA into nanoparticles and that enable cell membrane penetration with subsequent gene delivery to the nucleus has attracted much interest as an alternative to viral delivery.[1−6] In particular, liposomes composed of cationic lipids (CLs)[7−9] as well as synthetic polycations like poly(ethylenimine) (PEI) or α-poly(L-lysine) (PLL) and other cationic peptides[10,11] were greatly studied. Attention has been directed at the evaluation and understanding of the physicochemical properties of these DNA nanoparticles and the correlation of this data with transfection potency for various systems.[5,12−20] Information on particle size and surface charge can lead to further understanding and subsequent improvement of the formulations.[5,12−17,20] X-ray scattering has proven to be especially valuable in the determination of the supramolecular structure of the lipid/DNA complexes as pioneered in work by Safinya and coworkers.[9,13,21,22]

Huang and coworkers introduced the combination of liposomes with cationic peptides such as α-poly(L-lysine) to form a ternary complex of liposome/peptide/DNA (LPD).[23,24] This resulted in amplification of transfection as further demonstrated in subsequent work.[10,20,25] Additional argument in favor of a combined use of lipids and cationic peptides is related to the possibility to increase the versatility of the combined vectors.

The information on the physicochemical properties of these ternary lipid/peptide/DNA complexes and the relation of the physicochemical properties to transfection enhancement is still very limited. Previously, lipoplexes (lipid/DNA condensed structures) were extensively studied by synchrotron small-angle X-ray scattering (SAXS) to characterize the interaction between the DNA and lipids.[9,13,21,22] These studies showed that DNA and lipids were orderly organized in the complex and the phase of complex influenced the gene delivery process.[9,13,21,22] However, little information is available about the structures of ternary LPD complexes of lipid/peptide/DNA.

In a previous study,[26] the design and characterization of gene transfer vectors based on ε-oligolysines (Figure 1) was motivated by their favorable physical and biological properties being soluble, biodegradable, and nontoxic and by improved transfection compared with peptides such as α-poly-(L-lysine).[26,27]

Received: September 29, 2011
Published: November 9, 2011

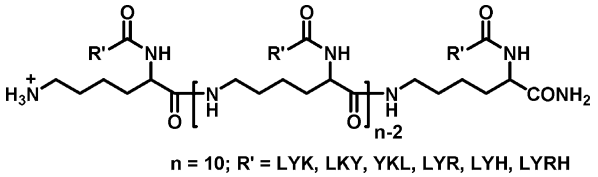

Figure 1. Chemical structure of α-substituted derivatives of ε-oligolysine studied in this work. The side chain of the ε-oligolysine decamer is formed by short α-peptides containing leucine (L), tyrosine (Y), lysine (K), arginine (R), and histidine (H).

In the present work, we have focused on establishing correlations between the enhanced transfection and the physicochemical properties of ternary self-assembled complexes of liposome/ε-peptide/DNA. The in vitro transfection efficiency in several cell lines and the particle sizes as well as zeta potentials of the nanoparticles formed in mixtures consisting of the lipid DOTAP (*N*-[1-(2,3-dioleoyloxy)propyl]-*N*,*N*,*N*-trimethylammonium methylsulfate), the gene-carrying plasmid DNA, and ε-oligolysines (Figure 1) was extensively characterized. This study extended to previous work and tested a range of formulations to identify conditions of optimal efficiency. We synthesized the novel peptides ε-(LYRH)K10, ε-(LYH)K10, ε-(LYK)K10, ε-(LKY)K10, and ε-(YKL)K10 and studied transfection in comparison with the previously studied ε-(LYR)K10. Histidine-containing peptides were investigated based on the reported facilitation of gene transfer caused by the enhancement of DNA endosomal escape through the "proton sponge" effect of the imidazole group of histidine.[4,10,28−30] We reasoned that the presence of both His and Arg in the ε-(LYRH)K10 may combine advantages of these two amino acids found in different transfection studies.

We performed SAXS measurements, which revealed that the three components, lipid, peptide, and DNA, self-assemble to multilamellar particles. DNA is arranged in parallel strands, sandwiched between the lipid bilayers with the peptides intercalated between DNA molecules, as illustrated in Figure 2.

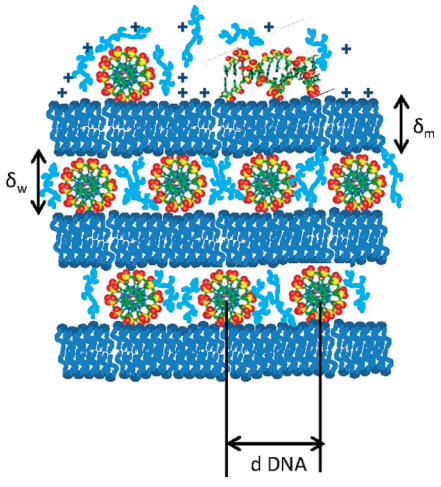

Figure 2. Schematic picture illustrating the lamellar phase of DOTAP/ε-peptide/DNA complexes, with alternating lipid bilayers and DNA monolayers. Peptides are arranged between DNA chains within the DNA monolayers. The DNA interaxial spacing is d_{DNA}. The interlayer spacing is $d = \delta_m + \delta_w$.

This structural organization suggests the roles of the peptides in the lipid/peptide/DNA complex, that is, acting as a DNA condensing agent with DOTAP and as a supplementary component for DNA protection, acting as a follow-on transfection vector after the malfunction of DOTAP. To the best of our knowledge, this is the first investigation of the supramolecular structure of these ternary complexes, and it demonstrates an interesting and novel self-assembly behavior of the lipid/cationic peptide/DNA system in aqueous solvent that suggests its mechanistic route in delivery.

The present lipid/peptide/DNA transfection system, based on ε-peptides, forms the basis for further optimization of transfection properties by the use of more effective liposomes and by further optimization of the peptide side chain, for example, by the inclusion of a nuclear localization signal sequence or receptor-targeting sequences.

MATERIALS AND METHODS

Materials. *DNA.* The plasmid pEGFP-N1 (4.7 kbp), which encodes the green fluorescent protein (GFP) was used. The plasmid was amplified in the *E. coli* DH5α strain and isolated using the QIAGEN (Valencia, CA) HiSpeed plasmid purification maxi kit or by the alkaline lysis method.

Peptides. α-Substituted ε-peptides ε-(LYK)K10, ε-(LKY)K10, ε-(YKL)K10, ε-(LYH)K10, ε-(LYRH)K10, and ε-(LYR)K10 (chemical structure is shown in Figure 1) were synthesized using solid-phase synthesis as described in detail in our previous work.[26] The peptide stock solutions (5 mg/mL; for SAXS samples it is 25 mg/mL) were prepared in sterile, double-distilled water.

Cell Culture. Hela human cervical carcinoma cells (CCL-2), 293F human embryonic kidney cells (PEAKrapid, CRL-2828), Mewo human melanoma cells (HTB-65), and A549 human lung carcinoma (CCL-185) were purchased from ATCC (Manassas, VA). Cells were grown in Dulbecco's modified Eagle's medium (DMEM; Gibco, Eggenstein, Germany) supplemented with 10% fetal bovine serum (FBS; Hyclone) at 37 °C in a humidified 5% CO_2 atmosphere. The cells were fed every 2 to 3 days and split when almost confluent employing tripsin/EDTA (Gibco).

Chemical Reagents. Transfection agent DOTAP (*N*-[1-(2,3-dioleoyloxy)propyl]-*N*,*N*,*N*-trimethylammonium methylsulfate, 1 mg/mL) solution was purchased from Roche (Basel, Switzerland). DOTAP lipids for SAXS samples were purchased from Avanti Polar Lipids (Alabaster, AL). DMSO and MTT (3-(4,5-dimethylthiazol-2-yl)-2,5-diphenyl tetrazolium bromide) were purchased from Sigma-Aldrich (St. Louis, MO). All other chemicals for buffers were purchased from Fisher Scientific (Pittsburgh, PA).

In Vitro Transfection, Flow Cytometry Analysis, and Cytotoxicity Assay. Preparation and measurements were carried out as in our previous work[26] with some modifications. The detailed description of experimental techniques is given in the Supporting Information.

Light Scattering and Zeta-Potential Measurements. Static (SLS) and dynamic (DLS) light scattering measurements were performed as previously described[26,27] with some modifications; detailed descriptions are given in the Supporting Information.

Particle size and zeta potential were measured at 25 °C using a Malvern Zetasizer Nano (Malvern Instruments, Worcestershire, U.K.) with a laser source operating at a wavelength of 633 nm. Samples were prepared in a volume of 1 mL and in buffer mimicking the conditions of the transfection studies (25 mM Hepes buffer pH 7.05 containing 70 mM NaCl and 0.75 mM Na_2HPO_4). For particle size measurement, light scattered by the sample was detected at an angle of 173° and Z-average diameters corresponding to scattering intensities were determined by applying standard theory using software provided by equipment manufacturer. For zeta potential (ζ) measurement, light scattered by the sample was detected at an angle of 17° and zeta potential values were calculated from measured velocities using the Smoluchowski model.

Small-Angle X-ray Scattering (SAXS). *Preparation of Liposomes.* DOTAP suspension in chloroform (Avanti Polar Lipids) was

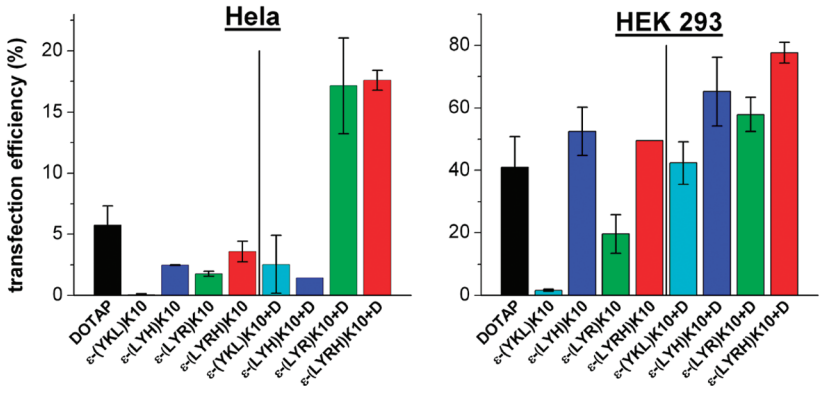

Figure 3. Transfection efficiencies of DOTAP, ε-(YKL)K10 ε-(LYH)K10, ε-(LYR)K10, ε-(LYRH)K10, and mixtures DOTAP-peptide determined for the Hela and HEK293 cell lines (indicated in the graphs). Transfection efficiency (mean value of three to five measurements with standard deviation) was measured as the ratio of the number of cells expressing GFP to the number of cells analyzed by flow cytometry. The black vertical bar separates data for peptides and mixtures of peptide + DOTAP.

dried under vacuum at room temperature for 1 h and dissolved in deionized water to concentration 25 mg/mL. Resuspended DOTAP was either extruded by LiposoFast-Basic with 100 nm polycarbonate membrane (Avestin, Canada) or sonicated with 1 s pulse of 30% amplitude for 10−15 min to clarity by tip sonicator Sonics vibra cell (Sonics & Materials, Newtown, CT, USA). The freshly prepared DOTAP (hydrodynamic diameter of ∼100 nm and polydispersity of ∼0.1 according to DLS measurement) was stored at room temperature.

SAXS Measurements. The mixture of peptide and DOTAP or pure DOTAP (control) in 75 μL of HBS buffer (25 mM Hepes, pH 7.05, 70 mM NaCl, and 0.75 mM Na_2HPO_4) was added to 100 μg plasmid DNA in 75 μL of HBS buffer to form complexes at the charge ratio of DOTAP to DNA (L/D) of 2.0 and charge ratios of peptide to DNA (P/D) varing from 0.3 to 5. Mixtures were sealed in 2 mm quartz capillaries (Charles Supper, Natick, MA) and centrifuged to force precipitates to pellet at the bottom of cappillaries. SAXS experiments were performed with 14.0 keV (λ = 0.886 Å) at the Beamline 23A SWAXS endstation at the National Synchrotron Radiation Research Center (Hsinchu, Taiwan).[31] Data were recorded by a charge-coupled device-based area detector (MarCCD165, Mar Evanston, IL) at 1.75 m sample-to-detector distance. The scattering wave vector $q = 4\pi\lambda^{-1} \sin\theta$ (with 2θ the scattering angle) was calibrated using silver behenate. SAXS profiles were circularly averaged from the isotropic 2-D patterns measured. All SAXS data were corrected for background scattering and sample transmission. The ordered distance d was calculated fron the q value of the corresponding peak using the relation $d = 2\pi/q$.

RESULTS AND DISCUSSION

In Vitro Transfection. The transfection abilities of the peptides ε-(YKL)K10, ε-(LYH)K10, ε-(LYR)K10, and ε-(LYRH)K10 and their mixtures with DOTAP (indicated as "peptide+D" in Figure 3) were examined for four cell lines. (Results were also compared with the peptides ε-(LYK)K10, ε-(LKY)K10; data not shown.) Figure 3 shows transfection results for the Hela and HEK 293 cells, which are commonly used in transfection studies. Figure S1 in the Supporting Information presents the results obtained for the A549 and Mewo cells that have been tested to compare transfection for cells with different surface receptors. In most of the experiments, we used the optimal peptide/DNA and DOTAP/peptides/DNA stoichiometry determined in our previous study.[26] The choice of the commercial transfection agent DOTAP as a control lipofection system is motivated by the fact that the characteristics and supramolecular properties of this transfection agent are well-studied,[2] and its chemical composition is known (unlike other commercial transfection products, e.g., Lipofectamine 2000), which is a necessity in physicochemical studies. Representative fluorescence images showing expression of GFP in Hela cells following transfection are shown in Figure S2 of the Supporting Information.

Figure 3 shows that in complexes of peptide and DNA, ε-(YKL)K10 was capable of delivering plasmid DNA to the nuclei, but the efficiency is low. Transfection was not detected for the peptides ε-(LYK)K10 or ε-(LKY)K10 (data not shown). It is observed that ε-(LYH)K10 and ε-(LYRH)K10 were more effective than DOTAP in HEK 293 cells (Figure 3). Arginine- or histidine-containing branches are more effective than those containing lysine, which is also observed for the combination with DOTAP (indicated as "peptide+D" in Figure 3). For the complex of the lipid DOTAP, peptide, and DNA (LPD complexes), the peptides ε-(LYR)K10 and ε-(LYRH)K10 produced an additive effect whereby the transfection of the LPD recipe exceeded that of the positive control (indicated as "DOTAP" in Figure 3) in both cell lines.

Those data confirm the improved transfection ability of the mixture DOTAP/peptide over DOTAP. In Hela cells, only ε-(LYR)K10 or ε-(LYRH)K10 improved transfection, and the effect of combination of DOTAP with either of these two peptides is significant (∼3.1 fold increased transfection). Similar transfection studies were done with A549 and Mewo cells, and the results (Supporting Information, Figure S1) were consistent with the data of HEK 293 and Hela cells.

Comparison of transfection efficiencies induced by ε-(LYK)-K10 and ε-(LYR)K10 demonstrates that gene expression is greatly increased when lysine in the side chain is substituted by arginine. The advantage of Arg over Lys residue was reported for protamine molecule mediated transfection.[24] Although Lys and Arg have many similar properties, a specific role of arginine was found in cell membrane translocation, which could account for the transfection ability.[32,33]

A rationale for including the histidine residues in cationic peptides for improved delivery is based on the "proton sponge" hypothesis. This effect is believed to be caused by protonation of the histidine in the endosomal pH, thereby absorbing protons of the lumen of the endosomes, acting as a "proton sponge". This in turn leads to an influx of chloride counterions, which raises the osmotic pressure and eventually causes endosomal swelling and DNA release.[4,10,28−30] The low pH in the endosomes may additionally promote the condensation ability of the polycationic peptide and further protect DNA.[4] We investigated the DNA condensation by the ε-oligolysines in

dx.doi.org/10.1021/bm201359r | *Biomacromolecules* 2012, 13, 124−131

various buffer environment (data shown in Figure S3, Supporting Information). The results showed that upon lowering pH from 7.5 to 5 (similar to that in the endosomes), the efficiency of the histidine-containing peptide in inducing DNA condensation is increased by more than 10 times. This can be explained by the increase in the positive charge of the ε-(LYH)K10 due to protonation of the imidazole side chain group of histidine ($pK_a \approx 6.5$).

The ε-(LYRH)K10 combining both Arg and His residues showed the best transfection in HEK 293 and Hela cells (Figure 3). The result indicates that multiple advantageous components for transfection can be integrated into a single peptide by using our ε-oligolysine backbone design.

Evaluation of Cytotoxicity. The cytotoxicity of individual peptides and binary peptide/DOTAP mixtures at the doses similar to that applied in the transfection study (shown in Figure 3) was evaluated by the MTT assay. Results are displayed in Figure 4. Exposure to ε-(LYK)K10 and

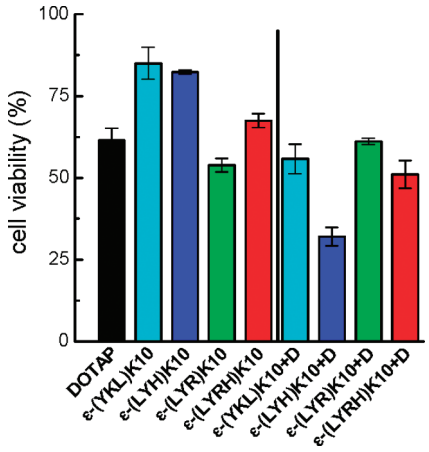

Figure 4. Hela cell viability after the treatment with DOTAP, ε-(YKL)K10, ε-(LYH)K10, ε-(LYR)K10, ε-(LYRH)K10, and mixtures DOTAP-peptide at the same concentration as we used in cell transfection. (Viability is shown as mean value of three to five measurements with standard deviation.) The black vertical bar separates data for peptides and mixtures of peptide + DOTAP.

ε-(LYH)K10 results in cell viability over 80%. DOTAP, ε-(LYR)K10, and ε-(LYRH)K10 display 50−70% cell viability, revealing moderate cytotoxicity. Similar or higher cell viabilities are also observed for the mixture peptide/DOTAP, with an exception of ε-(LYH)K10/DOTAP (30% cell viability).

The Arg- and His-containing peptides, ε-(LYH)K10, ε-(LYR)K10, and ε-(LYRH)K10, are promising gene delivery vectors in view of their transfection and cytotoxicity data. When ε-(LYR)K10 or ε-(LYRH)K10 is combined with DOTAP, enhanced transfection is observed with cytotoxicity level (50−70%) being only slightly worse than that displayed by the commercial transfection agent, DOTAP (∼60%).

Correlations between Transfection Abilities and Physicochemical Properties. According to the data shown in Figure 3, the branched ε-oligolysines enhanced DOTAP-mediated transfection as cotransfection agents. To study the formulation dependence of the potentiating effect, we measured transfection abilities of the ternary complexes DOTAP/peptide/DNA in Hela cells with various peptide concentrations using the most effective peptides ε-(LYH)K10, ε-(LYR)K10, and ε-(LYRH)K10. In parallel, particle size and zeta potential of the complexes were investigated to find correlations with transfection data and to explain the potentiating effect of the peptides in the LPD complexes. One of the major determinants of transfection properties is the charge ratio between the compaction agent and DNA.[14] Transfection complexes were prepared at constant DOTAP to DNA charge ratio, L/D = 2, varying the peptide to DNA charge ratio, P/D. Complexes of DOTAP/DNA at L/D = 2 were used as a control, and corresponding data points are drawn at P/D = 0 in Figure 5.

Figure 5 combines the results from transfection with data on zeta potential (Figure 5A) and particle size (Figure 5B). The black lines represent the transfection efficiency of the control complex DOTAP/DNA. Thus, the transfection data above the black lines indicate enhanced transfection relative to the DOTAP/DNA control. Figure 5 shows that significant enhancement in transfection was observed at high peptide-to-DNA charge ratio exceeding 5 for the complexes of the two peptides, ε-(LYR)K10 and ε-(LYRH)K10.

First, we discuss zeta potential measurements and the correlation of these results with transfection. The complex of DOTAP/ε-(LYRH)K10/DNA and DOTAP/ε-(LYR)K10/DNA had positive zeta potentials of ∼+16 mV at P/D = 1. It increased to ∼+20 mV with further increase in P/D (Figure 5A). The zeta potential of the DOTAP/ε-(LYH)K10/DNA complex was close to zero in the range of P/D = 1 to 10. This indicates that for a given peptide/DNA charge ratio the zeta potential is influenced by the peptide composition. However, an addition of peptides always resulted in a shift of the potential to more positive values relative to the control complex DOTAP/DNA, which has a zeta potential of −30.4 ± 0.8 mV. This observation demonstrates an inclusion of the positively charged peptides in the transfection complexes.

It was reported that at low concentration of salt, particles formed by interaction of CL and DNA are positively charged at CR > 1.[34] However, in salt solution mimicking conditions of transfection studies (25 mM Hepes, pH 7.05, 70 mM NaCl, and 0.75 mM Na_2HPO_4), complexes of DNA with cationic vectors have negative zeta potential.[20,25,35] This difference in sign of the zeta potential is explained by competition between lipids and monovalent cations for neutralization of the negative charge of the DNA absorbed on the surface of the particles. Under low salt conditions, there is little competition between lipids and Na^+ for the binding to DNA. Hence, DNA absorbed on the surface of the LD particles cannot reverse the overall positive charge of the L/D complex (because lipid is present in excess). However, at ∼70 mM Na^+ in HBS buffer, the competition with Na^+ weakens the ionic lipid−DNA interaction and results in the release the excessive lipid from the DNA absorbed on the surface so the zeta potential becomes negative. The ε-oligolysines used in the present study carry a high positive charge (+21), and according to our previous data,[36] when the peptides are added, 70 mM Na^+ is not enough to compete with ε-oligolysine for the binding to DNA The above consideration explains the observed value of about −30 mV for our control system DOTAP/DNA measured in HBS buffer.

The observed increase in zeta potential correlates with the augmentation of transfection (Figure 5A). For the DOTAP/peptide/DNA complexes, enhanced transfection is observed when the zeta potential is above +20 mV (this threshold potential is indicated by blue dash line; Figure 5A). It is known that zeta potential of the transfection complexes correlates with their affinity for the charged cell surfaces and a positive value of

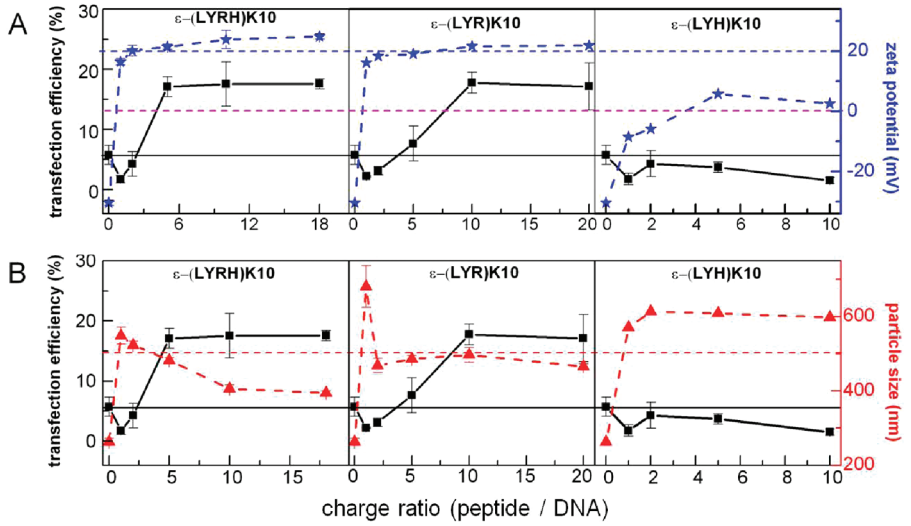

Figure 5. Comparison of transfection efficiency (black lines and symbols in all graphs) with zeta potential (panels A, blue lines and symbols) and with particle size (panels B, red lines and symbols) plotted as a function of peptide to DNA charge ratio for ternary complex of DOTAP/peptide/DNA containing peptide ε-(LYRH)K10, ε-(LYR)K10, or ε-(LYH)K10 (indicated in the graphs). The black horizontal lines marks transfection efficiency of the control complex DOTAP/DNA; blue dashed line in panel A indicates zeta potential of +20 mV; red dashed line in panel B shows particle size 500 nm. For the ternary complex of DOTAP/peptide/DNA, the charge ratio of DOTAP to DNA is constant and equal to 2. Components were mixed in HBS buffer (25 mM HEPES, pH 7.05, 70 mM NaCl, 0.75 mM Na_2HPO_4). All data are mean values of three to five measurements with standard deviation.

zeta potential is essential for effective transfection.[14] This explains the potentiating effect of peptide addition to the DNA/DOTAP mixtures observed in our study.

Next, we consider dependences of the particle size on peptide to DNA charge ratio and relation of this parameter to the transfection efficiency (Figure 5B). As concerns variations of particle size related to the addition of copolymers to the DNA/lipid recipes, results reported in literature are contradictory.[10,23,25] It was found that the addition of poly(L-lysine) or branched histidine-lysine copolymers to cationic liposome/DNA mixtures reduced the particle size,[10,23] whereas addition of HIV-1 Tat protein transduction domain peptide enlarged it.[25]

Our data show that all peptides drastically increased the size of the control complex DOTAP/DNA at P/D = 1, with no additional increase observed for P/D > 2. At all studied charge ratios, we observed that the sizes of DOTAP/ε-peptide/DNA complexes are larger than those of DOTAP/DNA (Figure 5B). A decrease in the particle size is seen with increase in peptide/DNA charge ratio for complexes DOTAP/ε-(LYRH)K10/DNA and DOTAP/ε-(LYR)K10/DNA. Considering individual peptides, it is observed that ε-(LYH)K10 forms larger particles (~600 nm) than ε-(LYRH)K10 and ε-(LYR)K10 (Figure 5 B). The size of the particles is related to the zeta potential because particles tend to repel each other when their surface charges (represented by zeta potential) are high; otherwise, they are more likely to form aggregates with large diameters. The correlation between particle size and zeta potential is evident by plotting sizes and absolute values of zeta potential against the charge ratio (Figure S4, Supporting Information).

We observed that the efficiency of transfection increases with decrease in the particle size. This sort of correlation (smaller size—higher efficiency) was reported in many other studies (e.g., refs 10 and 23). However, not only particle size but also the presence of oligopeptide is important because most effective LPD complexes are larger than those composed of DOTAP/DNA.

To summarize, we found that for the ternary DOTAP/ε-oligolysine/DNA complexes, enhanced transfection is observed when the zeta potential is above +20 mV. (This threshold potential is indicated by the blue dashed line (Figure 5A).) As concerns the effect of particle size, enhancement of transfection is seen when the sizes are <500 nm (red points below red dashed lines in Figure 5B).

Supramolecular Structure. The supramolecular structures of the transfection complexes for mixtures of DOTAP/ε-(LYR)K10/DNA and DOTAP/ε-(LYRH)K10/DNA at a lipid to DNA ratio, L/D = 2, with variations of P/D were investigated by synchrotron SAXS, and spectra are shown in Figure 6. Spectral characteristics and structural parameters are assembled in Table 1. The complex of DOTAP/DNA at L/D = 2 was examined as a reference (upper black curve in Figure 6A,B). The spectrum for this control system has been greatly studied and may serve as an illustration of the typical behavior for the formation of multilamellar bilayers with parallel DNA strands intercalated in the aqueous region between bilayers. The multilamellar structure gives rise to lamellar peaks that follow the relation $d = 2\pi n/q_{00n}$.[22] The integer n = 1, 2, 3, ... denotes the Bragg peaks, q_{00n}, of various order n. In the spectra shown in Figure 6, only the peaks corresponding to n = 1 and 2, denoted q_{001} and q_{002} and indicated by black arrows, are of sufficient intensity to be visible. Here d is the interlayer distance and with q_{001} = 0.103 (Table 1); the observed interlamellar spacing of 61 Å is consistent with one aqueous layer including the double helical DNA, where $d = \delta_w + \delta_m$. Here δ_w, the aqueous layer including DNA, is expected to be ~24 Å in diameter, and the thickness of a bilayer of pure DOTAP, δ_m, is ~37 Å.[22] (See Figure 2 for a general illustration.)

In addition, the control DOTAP/DNA system shows a peak interpreted as due to DNA helices arranged in parallel within the aqueous region between the bilayers.[22] (See the top black curves in Figure 6, indicated by pink arrows.) From a relation similar to the one given above and used to obtain the multilamellar repeat distance, the DNA—DNA correlation

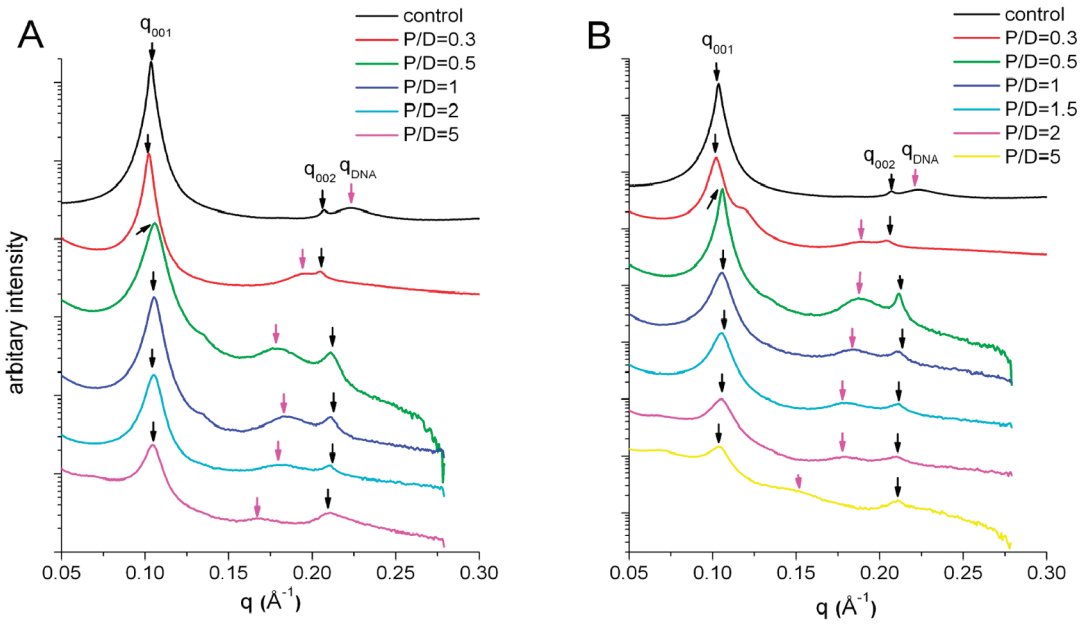

Figure 6. SAXS spectra of (A) DOTAP/ε-(LYR)K10/DNA and (B) DOTAP/ε-(LYRH)K10/DNA complexes at L/D = 2 in HBS buffer (25 mM HEPES, pH 7.05, 70 mM NaCl, 0.75 mM Na_2HPO_4) as a function of peptide/DNA (P/D) charge ratio. Black arrows indicate the lamellar peaks; pink arrows show the DNA−DNA correlation peaks. The q values of lamellar (black numbers) and DNA−DNA correlation (pink numbers) peaks and the correponding distance are given in Table 1. The "control" is DOTAP/DNA complex at L/D = 2.

Table 1. Values of the Scattering Vector, q, for Peaks Observed in SAXS Spectra of the DOTAP/Peptides/DNA Mixtures with Varied Peptide to DNA (P/D) Charge Ratios and Corresponding Lamellar Repeat Distances, d, As Well As DNA−DNA Separations, d_{DNA}, Obtained from the Spectra[a]

L/D	P/D	q_{001} (Å^{-1})	q_{DNA} (Å^{-1})	q_{002} (Å^{-1})	d, interlamellar (Å)	d_{DNA} (Å)
2	5	0.104	0.168	0.21	60.4	37.4
2	0	0.103	0.22	0.206	61	28.6
2	0.3	0.102	0.196	0.205	61.6	32
2	0.5	0.105	0.178	0.211	59.8	35.3
2	1	0.105	0.184	0.211	59.9	34
2	2	0.105	0.182	0.211	59.8	34.5
L/D	P/D	q_{001} (Å^{-1})	q_{DNA} (Å^{-1})	q_{002} (Å^{-1})	d, interlamellar (Å)	d_{DNA} (Å)
2	0	0.103	0.22	0.206	61	28.6
2	0.3	0.102	0.188	0.204	61.6	33.4
2	0.5	0.106	0.188	0.211	59.3	33.4
2	1	0.105	0.185	0.211	59.8	34
2	1.5	0.105	0.179	0.211	59.8	35.1
2	2	0.105	0.178	0.21	59.8	35.3
2	5	0.104	0.15	0.21	60.4	41.9

[a] q and distance values are from the synchrotron SAXS spectra shown in Figure 6A,B, respectively.

distance, d_{DNA}, is obtained ($d_{DNA} = 2\pi/q_{DNA}$). The control DOTAP/DNA complex shows a high DNA packing density with a DNA−DNA distance of ∼29 Å (obtained from q_{DNA} = 0.22; see Table 1). This is in agreement with literature data for DOTAP/DNA complexes.[2] This DNA−DNA distance is slightly larger than the hydrated diameter of DNA (∼24 Å).

Table 1 summarizes the observed spectral parameters and lamellar repeat distances, d, as well as DNA−DNA separations, d_{DNA}, obtained from the spectra in Figure 6. All ternary lipid/peptide/DNA complexes showed spectra corresponding to typical lamellar phases with peak positions and interlayer spacing similar to the DOTAP/DNA control (59.3 to 61.6 Å; see Table 1). The positions of the lamellar peaks do not depend on the peptide nature, as illustrated by the similar features of the results comparing ε-(LYR)K10 results in Figure 6A and ε-(LYRH)K10 data in Figure 6B. (See also Table 1A.) The formation of multilamellar structure also does not depend on the peptide/DNA ratio, as illustrated by comparison of the spectra in Figure 6 and parameters in Table 1 (increasing peptide concentration from top to bottom in Figure 6). With the observed multilamellar distance being ∼61 Å, which is the same as the peptide-free DOTAP/DNA control, there is no space between DNA and lipids to accommodate the peptide molecules.

In addition, the peak corresponding to the DNA−DNA correlation distance, d_{DNA}, is also present in the ternary complexes. These observations demonstrate self-assembly to multilamellar LPD complexes with the arrangement of DNA in between the bilayers, similar to that of the DNA-DOTAP lipid control.

From the relation $d_{DNA} = 2\pi/q_{DNA}$, we can extract the DNA−DNA separation in the ternary DOTAP/ε-lysine/DNA complexes and the results are compiled in Table 1. Interestingly, the distance between the DNA rods, increases when peptide is added to the DOTAP/DNA system, being about 32−33 Å for the lowest peptide/DNA ratio of P/D = 0.3 (compared with ∼29 Å for the control in absence of peptide, see Table 1). With increase of peptide concentration, from P/D = 0.3 to P/D = 5, the DNA−DNA correlation peaks shifts to lower q (Å^{-1}) values, correponding to an increase of d_{DNA}, with the ε-(LYRH)K10 system having an inter-rod DNA−DNA separation of ∼41 Å at P/D = 5 (Table 1). Thus, compared to the control DOTAP/DNA complex, d_{DNA} increases by around 10 Å at P/D = 5. Increase in d_{DNA} upon increase in CR was also observed in lipid/DNA mixtures (where either CL or its

dx.doi.org/10.1021/bm201359r | Biomacromolecules 2012, 13, 124−131

mixture with neutral lipids was used).[34] This effect can be explained by a tendency of DNA to interact electrostatically with a maximum amount of positive charge (no matter if this increase is created by addition of e-oligolysines as in this work or by increase in CL in the mixture of lipids).[34]

Indeed, a thermodynamic analysis of nonstoichiometric mixtures of polyanions (DNA) and polycations explains this behavior. (ε-oligolysines and CLs in bilayer or in liposome form can be considered as a polycation.). Under nonstoichiometric conditions (when the charge ratio is not equal to 1.0), electrostatic interactions of all polycations with all polyanions are more favorable than the situation when the charge of the polyanion is exactly balanced by the cationic ligand, with any excess of oligocations being free (not interacting with DNA). The origin of this effect is entropic. It appears that total release of monovalent counterions is larger when the charge density of all polyionic species is reduced compared with the counterion release observed upon formation of 1:1 DNA:polycation (or lipid) complex with excess polycations remaining free. This effect was discussed in detail for polycation−DNA systems.[37,38]

A plausible explanation of the origin of the increase in the in-plane DNA−DNA distance with the increase in peptide content is that the peptide molecules infiltrate between the DNA−DNA layers in the aqueous phase between the bilayers and intercalate between DNA chains. The increased DNA−DNA distance is consistent with accommodation of peptides having a relatively thin ε-K10 backbone with a diameter of 3 to 4 Å and with the side chains somewhat penetrating into the DNA grooves as schematically illustrated in Figure 2. For the present lamellar systems, the data do therefore not support increased DNA condensation in the presence of the peptides[10,23] because the DNA chains in the LPD complexes were packed less tightly than in the DOTAP/DNA complex.

■ CONCLUSIONS

The data obtained in the present study confirm and extends the conclusion of previous work[26] that α-substituted ε-lysines are promising gene delivery vectors. The arginine/histidine-bearing peptides ε-(LYH)K10, ε-(LYR)K10, and ε-(LYRH)K10 show a potential of being successful DNA carriers compared with the peptides with lysine in the side chain (Figures 3 and 4). We observed that the ε-lysine-based peptides can act as effective coagents in DOTAP-mediated transfection; that is, peptide/DOTAP mixtures are more effective than DOTAP alone (Figure 3). The most significant enhancement of transfection was achieved when ε-(LYH)K10, ε-(LYR)K10, or ε-(LYRH)K10 was combined with DOTAP.

For the DOTAP/ε-peptide/DNA complexes, a universal optimal zeta potential (above +20 mV) and particle size (<500 nm) might serve as an important condition for effective transfection (Figure 5). As far as we know, this correlation has not previously been pointed out and analyzed in a systematic way by correlating these physicochemical properties with transfection. The SAXS data allowed us to conclude that self-assembly to a lamellar phase was spontaneously initiated for the ternary complexes DOTAP/ε-peptide/DNA (Figure 6). The peptides are distributed between the DNA rods in the water phase of lamella rather than between DOTAP and the DNA layers because there is no change in interlayer spacing with P/D variations (Figure 2).

The supramolecular structures formed by DNA condensed by the ε-peptides and DOTAP to form lamellar phases (as schematically shown in Figure 2) could ensure the synergistic effect of branched ε-oligolysines and DOTAP in transfection and suggests two major factors that may be responsible for it:

(1) Peptides covering the exposed DNA on the particle surface lead to a stronger cell association.
(2) Peptides distributed in the aqueous layer are associated with DNA molecules, which could work as an additional transfection vector.

It also suggests the mechanism underlying DNA transfer mediated by both DOTAP and ε-oligolysines. The function of DOTAP might be disturbed by membrane fusion or serum interference, especially during in vivo transfection.[15,21,39] Inclusion of the peptides into DOTAP/DNA complexes provides additional protection for DNA on a route from the extracellular solution to the cell nucleus. Peptides possibly assist gene delivery as follow-on vectors even after DOTAP coating is abolished, for example, by protecting DNA from digestion by DNase I in the cytosol. Because of the multiple barriers in the gene delivery process,[39] such organization may be significant for final successful gene expression.

■ ASSOCIATED CONTENT

Ⓢ Supporting Information

Experimental details and transfection efficiency graphs, fluoresence images, and influence of pH on DNA condensation and comparison absolute values of zeta potential with particle size plots. This material is available free of charge via the Internet at http://pubs.acs.org.

■ AUTHOR INFORMATION

Corresponding Author

*Tel: +65 6316-2812. Fax: +65 6795 3856. E-mail: LarsNor@ntu.edu.sg.

■ ACKNOWLEDGMENTS

This work was financially supported by the Singapore Agency for Science Technology and Research (A*STAR) BMRC (Biomedical Research Council) grant and by Singapore Ministry of Education (MOE) Tier 2 and ARC-Tier 1 grants. The National Synchrotron Radiation Research Center (NSRRC) at Hsinchu, Taiwan is acknowledged for generous allocation of beamtime that enabled the Synchrotron X-Ray scattering measurements. We are indebted to the Small/Wide Angle X-ray Scattering beamline staff for technical assistance.

■ REFERENCES

(1) Segura, T.; Shea, L. D. Materials for non-viral gene delivery. *Annu. Rev. Mater. Res.* **2001**, *31*, 25−46.
(2) Safinya, C. R. Structures of lipid−DNA complexes: supramolecular assembly and gene delivery. *Curr. Opin. Struct. Biol.* **2001**, *11*, 440−448.
(3) Liu, F.; Huang, L. Development of non-viral vectors for systemic gene delivery. *J. Controlled Release* **2002**, *78*, 259−266.
(4) Martin, M. E.; Rice, K. G. Peptide-guided gene delivery. *AAPS J.* **2007**, *9*, E18−E29.
(5) Gao, X.; Kim, K.-S.; Liu, D. Nonviral gene delivery: what we know and what is next. *AAPS J.* **2007**, *9*, E92−E104.
(6) Mintzer, M. A.; Simanek, E. E. Nonviral vectors for gene delivery. *Chem. Rev.* **2009**, *109*, 259−302.
(7) Hofland, H. E.; Shephard, L.; Sullivan, S. M. Formation of stable cationic lipid/DNA complexes for gene transfer. *Proc. Natl. Acad. Sci. U.S.A.* **1996**, *93*, 7305−7309.

(8) Lasic, D. D.; Strey, H.; Stuart, M. C. A.; Podgornik, R.; Frederik, P. M. The structure of DNA-liposome complexes. *J. Am. Chem. Soc.* **1997**, *119*, 832−833.
(9) Rädler, J. O.; Koltover, I.; Salditt, T.; Safinya, C. R. Structure of DNA−cationic liposome complexes: DNA intercalation in multilamellar membranes in distinct interhelical packing regimes. *Science* **1997**, *275*, 810−814.
(10) Chen, Q. R.; Zhang, L.; Stass, S. A.; Mixson, A. J. Branched co-polymers of histidine and lysine are efficienct carriers of plasmids. *Nucleic Acids Res.* **2001**, *29*, 1334−1340.
(11) Rudolph, C.; Plank, C.; Lausier, J.; Schillinger, U.; Muller, R. H.; Rosenecker, J. Oligomers of the arginine-rich motif of the HIV-1 TAT protein are capable of transferring plasmid DNA into cells. *J. Biol. Chem.* **2003**, *278*, 11411−11418.
(12) Ross, P. C.; Hui, S. W. Lipoplex size is a major determinant of in vitro lipofection efficiency. *Gene Ther.* **1999**, *6*, 651−659.
(13) Ewert, K.; Slack, N. L.; Ahmad, A.; Evans, H. M.; Lin, A. J.; Samuel, C. E.; Safinya, C. R. Cationic lipid-DNA complexes for gene therapy; understanding the relationship between complex structure and gene delivery pathways at the molecular level. *Curr. Med. Chem.* **2004**, *11*, 133−149.
(14) Rao, N. M.; Gopal, V. Cell biological and biophysical aspects of lipid-mediated gene delivery. *Biosci. Rep* **2006**, *26*, 301−324.
(15) Koynova, R.; Wang, L.; MacDonald, R. C. An intracellular lamellar−nonlamellar phase transition rationalizes the superior performance of some cationic lipid transfection agents. *Proc. Natl. Acad. Sci. U.S.A.* **2006**, *103*, 14373−14378.
(16) Marchini, C.; Montani, M.; Amici, A.; Amenitsch, H.; Marianecci, C.; Pozzi, D.; Caracciolo, G. Structural stability and increase in size rationalize the efficiency of lipoplexes in serum. *Langmuir* **2009**, *25*, 3013−3021.
(17) Le Bihan, O.; Chevre, R.; Mornet, S.; Garnier, B.; Pitard, B.; Lambert, O. Probing the in vitro mechanism of action of cationic lipid/DNA lipoplexes at a nanometric scale. *Nucleic Acids Res.* **2011**, *39*, 1595−1609.
(18) Duguid, J. G.; Li, C.; Shi, M.; Logan, M. J.; Alila, H.; Rolland, A.; Tomlinson, E.; Sparrow, J. T.; Smith, L. C. A physicochemical approach for predicting the effectiveness of peptide-based gene delivery systems for use in plasmid-based gene therapy. *Biophys. J.* **1998**, *74*, 2802−2814.
(19) Bello-Roufai, M.; Lambert, O.; Pitard, B. Relationships between the physicochemical properties of an amphiphilic triblock copolymers/DNA complexes and their intramuscular transfection efficiency. *Nucleic Acids Res.* **2007**, *35*, 728−739.
(20) Son, K. K.; Tkach, D.; Patel, D. H. Zeta potential of transfection complexes formed in serum-free medium can predict in vitro gene transfer efficiency of transfection reagents. *Biochim. Biophys. Acta* **2000**, *1468*, 11−14.
(21) Koltover, I.; Salditt, T.; Rädler, J. O.; Safinya, C. R. An inverted hexagonal phase of cationic liposome−DNA complexes related to DNA release and delivery. *Science* **1998**, *281*, 78−81.
(22) Rädler, J.; Koltover, I.; Jamieson, A.; Salditt, T.; Safinya, C. R. Structure and interfacial aspects of self-assembled cationic lipid-DNA gene carrier complexes. *Langmuir* **1998**, *14*, 4272−4283.
(23) Gao, X.; Huang, L. Potentiation of cationic liposome-mediated gene delivery by polycations. *Biochemistry* **1996**, *35*, 1027−1036.
(24) Sorgi, F. L.; Bhattacharya, S.; Huang, L. Protamine sulfate enhances lipid-mediated gene transfer. *Gene Ther.* **1997**, *4*, 961−968.
(25) Hyndman, L.; Lemoine, J. L.; Huang, L.; Porteous, D. J.; Boyd, A. C.; Nan, X. HIV-1 Tat protein transduction domain peptide facilitates gene transfer in combination with cationic liposomes. *J.Contr.Release* **2004**, *99*, 435−444.
(26) Huang, D.; Korolev, N.; Eom, K. D.; Tam, J. P.; Nordenskiöld, L. Design and biophysical characterization of novel polycationic ε-peptides for DNA compaction and delivery. *Biomacromolecules* **2008**, *9*, 321−330.
(27) Tam, J. P.; Lu, Y. A.; Yang, J. L. Antimicrobial dendrimeric peptides. *Eur. J. Biochem.* **2002**, *269*, 923−932.
(28) Chen, Q.-R.; Zhang, L.; Stass, S. A.; Mixson, A. J. Co-polymer of histidine and lysine markedly enhances transfection efficiency of liposomes. *Gene Ther.* **2000**, *7*, 1698−1705.
(29) Chen, Q. R.; Zhang, L.; Luther, P. W.; Mixson, A. J. Optimal transfection with the HK polymer depends on its degree of branching and the pH of endocytic vesicles. *Nucleic Acids Res.* **2002**, *30*, 1338−1345.
(30) Yu, W.; Pirollo, K. F.; Yu, B.; Rait, A.; Xiang, L.; Huang, W.; Zhou, Q.; Ertem, G.; Chang, E. H. Enhanced transfection efficiency of a systemically delivered tumor-targeting immunolipoplex by inclusion of a pH-sensitive histidylated oligolysine peptide. *Nucleic Acids Res.* **2004**, *32*, e48.
(31) Jeng, U. S.; Su, C. H.; Su, C. J.; Liao, K. F.; Chuang, W. T.; Lai, Y. H.; Chang, J. W.; Chen, Y. J.; Huang, Y. S.; Lee, M. T.; Yu, K. L.; Lin, J. M. A small/wide-angle X-ray scattering instrument for structural characterization of air-liquid interfaces, thin films and bulk specimens. *J. Appl. Crystallogr.* **2010**, *43*, 110−121.
(32) Futaki, S.; Suzuki, T.; Ohashi, W.; Yagami, T.; Tanaka, S.; Ueda, K.; Sugiura, Y. Arginine-rich peptides. An abundant source of membrane-permeable peptides having potential as carriers for intracellular protein delivery. *J. Biol. Chem.* **2001**, *276*, 5836−5840.
(33) Wender, P. A.; Mitchell, D. J.; Pattabiraman, K.; Pelkey, E. T.; Steinman, L.; Rothbard, J. B. The design, synthesis, and evaluation of molecules that enable or enhance cellular uptake: peptoid molecular transporters. *Proc. Natl. Acad. Sci. U.S.A.* **2000**, *97*, 13003−13008.
(34) Koltover, I.; Salditt, T.; Safinya, C. R. Phase diagram, stability, and overcharging of lamellar cationic lipid-DNA self-assembled complexes. *Biophys. J.* **1999**, *77*, 915−924.
(35) Li, D.; Ping, Y.; Xu, F.; Yu, H.; Pan, H.; Huang, H.; Wang, Q.; Tang, G.; Li, J. Construction of a star-shaped copolymer as a vector for FGF receptor-mediated gene delivery in vitro and in vivo. *Biomacromolecules* **2010**, *11*, 2221−2229.
(36) Korolev, N.; Berezhnoy, N. V.; Eom, K. D.; Tam, J. P.; Nordenskiöld, L. A universal description for the experimental behavior of salt-(in)dependent oligocation-induced DNA condensation. *Nucleic Acids Res.* **2009**, *37*, 7137−50.
(37) Korolev, N.; Lyubartsev, A. P.; Laaksonen, A. Electrostatic background of chromatin fiber stretching. *J. Biomol. Struct. Dyn.* **2004**, *22*, 215−226.
(38) Korolev, N.; Lyubartsev, A. P.; Nordenskiöld, L. Application of the Poisson Boltzmann polyelectrolyte model for thermal denaturation of DNA in the presence of Na^+ and polyamine cations. *Biophys. Chem.* **2003**, *104*, 55−66.
(39) Read, M. L.; Logan, A.; Seymour, L. W. Barriers to gene delivery using synthetic vectors. *Adv. Genet.* **2005**, *53PA*, 19−46.